Local tracer emission mimicking air-borne disease spreading in an office space with mixing ventilation

Mikael Björling [1,*]

[1] Department of Electrical engineering, Mathematics and Science, Faculty of Engineering and Sustainable Development, University of Gävle, Gävle, Sweden

[*] *Corresponding email: Mikael.Bjorling@hig.se*

SUMMARY
In a laboratory office setting with four occupants facing the walls, local emission of a tracer gas (B) in the breathing zone of one infected occupant mimics the transmission of an air-borne disease. At the same time, another tracer gas (A) is homogeneously emitted in the office space so that the local mean age can be determined in each sampling point. Tracers are passively collected in the breathing zones of the occupants and in sixteen sampling positions distributed at four heights. A laboratory office setup with mixing ventilation conditions and a single ceiling exhaust in a corner is investigated. The distribution of B-tracer is analyzed in the sampling points for the four possible locations of an infected occupant in relation to the exhaust location. The results reported are in the absence of thermal plumes, i.e., the manikins representing occupants were turned off. The relative apparent emission rates calculated from the measurements are conjectured to represent the steady state transfer probabilities from the respective breathing zones. As expected, for mixing ventilation conditions, the steady state probabilities to most positions are similar. Nevertheless, the steady state transfer probabilities from the breathing zones of the pair of manikins closer to the exhaust cause slightly more spreading, 0.83 ± 0.04 and 0.82 ± 0.04, than the other pair, 0.76 ± 0.03 and 0.75 ± 0.06.

KEYWORDS
air-borne disease transmission, office environment, mixing ventilation, local mean age of air.

1 INTRODUCTION
The occurrence of world-wide pandemics caused by virus infections are likely to happen again. It is now fairly well established that such infections are spreading via two routes (Wagner et al, 2021): a short-range route via face-to-face interactions important at distances < 1 m; and a long-range route dominated by aerosol transport. In the latter case, ventilation systems of an indoor environment may be both friend and foe. The ventilation system can either decrease aerosol exposure by diluting the indoor air or transporting it away but may also inadvertently contribute to increased spreading of the infectious aerosols. It is therefore of interest to examine in more detail how different ventilation systems interact with the presence of infectious occupants in the indoor environment. This is a complex task with many relevant parameters (see for example Kurnitsky et al, 2023; Zhang and Lin, 2021; Kabanshi et al, 2024).

This pilot study is focusing on one of them: the transfer probability of aerosol, by air movements, within an office space. While the temporal aspects of increasing transfer probability could provide societal guidelines concerning safe time limits for co-occupation of an office space with potentially infected persons, they are also more difficult to examine. The steady state transfer probabilities that establish after long times, in each given system, are somewhat more tractable to measure. The final aim of this pilot study is to do just that in a laboratory setup of a small office space with four occupants. The preliminary study reported

here attempts to establish the base conditions in the absence of thermal plumes but can also serve as a proof of concept.

2 METHOD

The laboratory setup is a room 4x4x2.5 meters with mixing ventilation delivered from a centrally located ceiling dispenser and a ceiling exhaust located in the corner as shown in Figure 1a. Four manikins are placed facing each of the four walls. Note however that the heat sources of the manikins are not turned on in the measurements reported here. The chosen ventilation rate is 5 Liters/s/person. The total flow at the inlet is 20 L· s^{-1} or 72 m^3· h^{-1}. This corresponds to a nominal time constant of 0.56 h and a nominal air change rate of 1.8 h^{-1}. Open globular structures are placed at a height of 1.1 meters in front of the manikins, representing the breathing zones of sitting occupants. Two different PFT-tracers (here denoted A and B) are used. Twelve A-sources are placed at 0.3, 0.9 and 1.5 meters above the floor on four strings (see Figure 1a for locations) to achieve approximately homogeneous emission in the room. They are used to measure the local mean age of air based on the ISO-standard, ISO 16000-8, "Determination of local mean ages of air in buildings for characterizing ventilation conditions". One B-source is deployed separately in the breathing zone of one manikin to mimic the location of an infected person. Temperature loggers are in the middle of the room and in the breathing zone where the B-source is placed. The temperatures varied between 24 °C to 26 °C. Before each of the four measurement sets, the B-source was moved to a new location and measurements were started after a waiting period of two to three hours. The total sampling time varied from 44 to 72 hours. The four measurement sets were performed in the following sequence: B in Red, B in Yellow, B in Green and B in Blue. Twenty samplers per measurement were placed at 0.5, 1.0, 1.5 and 2.0 meters above the floor on four strings and in each of the four breathing zones. See Figure 1 for sampler (measurement) positions.

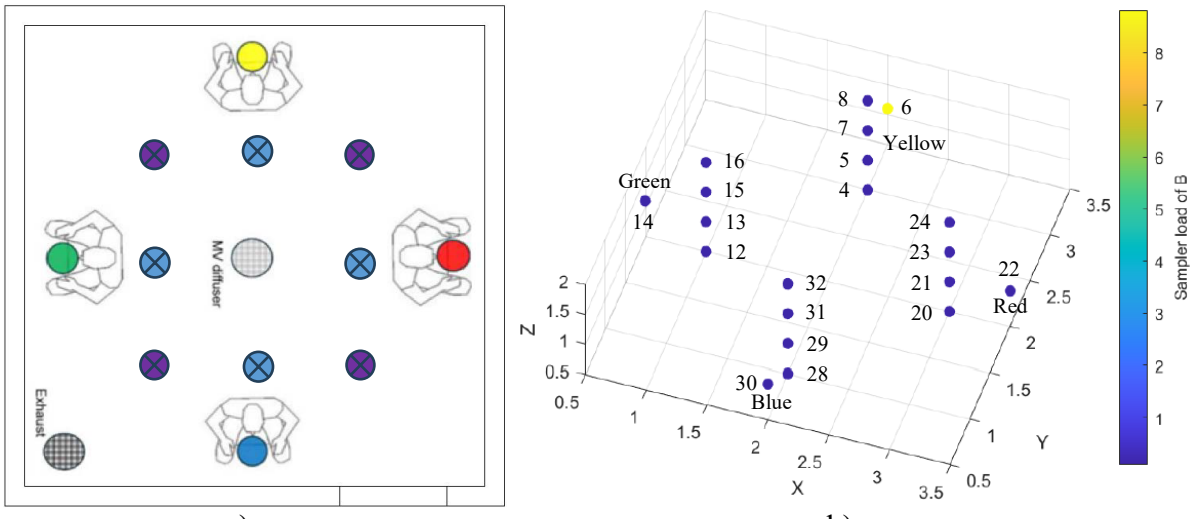

a) b)

Figure 1. Lab room setup. a) The X-direction is to the left and the Y-direction is up. Viewed from the top (Z-direction) showing the location of the manikins and their respective breathing zones. A-sources are located along the Z-direction in the violet points. Samplers are placed in the Z-direction (0.5, 1.0, 1.5 and 2.0 meters above the floor) located in the blue points and in the breathing zones (yellow, green, red, blue: 1.1 meters above the floor). b) 4-D visualization of the sampling positions. Example of results for the sampler load of tracer B, when a B-source is placed in the yellow breathing zone (B in Yellow). The numbers by the measurement position corresponds to the data point numbers in Figures 4-7.

3 THEORY

The measurements are based on the fact that the steady state concentration of a tracer (p) that is homogeneously emitted in the room is proportional to the local mean age of air and the emission rate per volume

$$c_p = \tau \cdot \frac{\dot{m}}{V}, \tag{1}$$

where c_p [kg m^{-3}] is the local steady state concentration of tracer, τ [h] is the local mean age of air, $\dot{m}$ [kg h^{-1}] is the constant emission rate of tracer and V [m^3] is the volume of the zone. The average local steady state concentration of tracer is given by

$$\langle c_p \rangle = \frac{M}{\omega \cdot T}, \tag{2}$$

where $\langle c_p \rangle$ [kg m^{-3}] is the average local steady state concentration of tracer in the sampling period, M [kg] is the sampler load of tracer, ω [m^3 h^{-1}] is the air sampling rate, T [h] is the sampling time. Since the emission of A-tracer approximately homogeneous in this measurement and the emission rate of A is known, an average local mean age of air $\langle \tau \rangle$ can be calculated using Eqs. 1 and 2.

A general model), originally proposed by Sandberg (1992), considers a much smaller volume element (i) of the room. The great advantage of the advanced model is that local sources and the possibility of stagnant zones within the room may be treated. In this context, the steady state concentration of any tracer becomes (see Etheridge and Sandberg, 1996 or Björling *et al*, 2011)

$$c_{i\infty} = \frac{\sum_j P_{ij} \dot{m}_j}{\sum_j P_{ij} Q_{js}} = \frac{S_i}{U_i} = \frac{S_i/V}{U_i/V} \approx \tau_i \frac{S_i}{V}, \tag{3}$$

where P_{ij} is the steady state transfer probability from volume element j to volume element i, Q_{js} is the clean purging air flow from the surroundings (i.e. inlet) to the volume element j, S_i is the local apparent emission rate of pollutant, U_i is the local purging flow, V [m^3] is the volume of the room, τ_i [h] is the local mean age of air in i. The latter approximate equality is the conjecture that the specific air change rate N_i (see Sandberg, 1992) is related to the inverse of τ_i so that

$$N_i = \frac{U_i}{V} = \frac{1}{\tau_i} \approx \frac{1}{\langle \tau_i \rangle}. \tag{4}$$

Consequently, by deploying a single B source with a known emission rate in a breathing zone the transfer probabilities to the other measuring points can be determined using Eqs. 1–4. Clearly, U_i, τ_i and N_i (measured using tracer A) are independent of the tracer gas used. Using a single source B in volume element k, S_i in Eq. 3 collapses into a single term $S_i = P_{ik} \dot{m}_k^B$. By determining the concentration $c_{i\infty}$ of tracer B and dividing by the known emission rate of a tracer B source, the relative apparent emission of tracer B in volume element i, coming from the single source placed in k., can be determined. If the conjecture is correct, this is equivalent to the transfer probability P_{ik} and can be universally used in calculations of infection spreading by aerosol transport for different emission rates of pathogens from k to i.

4 RESULTS AND DISCUSSION

Examples of results for the local mean age of air are presented in Figure 2. In the left plot, from the very first measurement, the results air seems older towards the exhaust in the ceiling in the left-hand corner. In the plot on the right side, from the third measurement, the values for the local mean ages of air are less scattered. The relative standard error in the measurements is approximately 10 %, mainly because of the relative standard error in the sample loads that is estimated to be no greater than 5%.

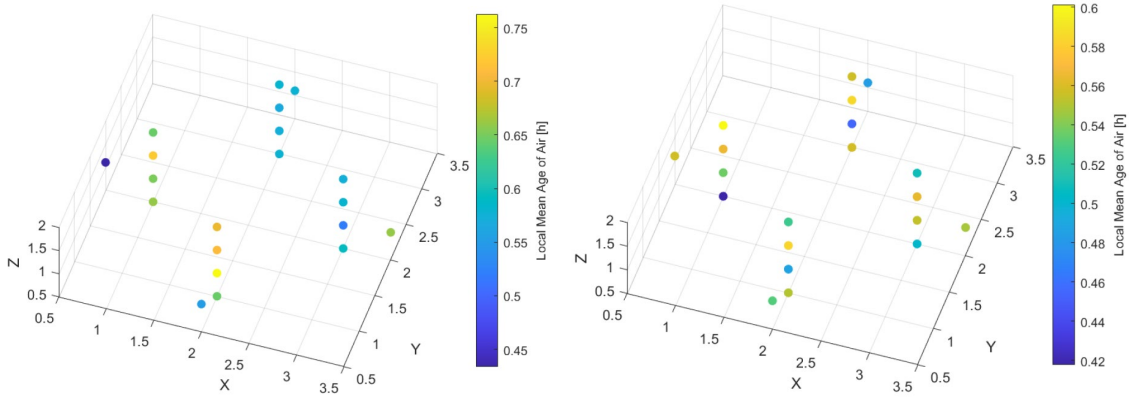

Figure 2. The measured local mean age of air for the first measurement (B in Red, left) and the third measurement (B in Green, right). Note that the sampling points in the breathing zones are all at 1.1 m above the floor even though the chosen viewpoint makes this less clear.

Because of the mixing ventilation conditions, fairly uniform results are expected. The biased results in the left plot may be explained by a too short waiting time before the measurements started. Perhaps this time was not sufficiently allowing for equilibration of the A-tracer in the room. For the third measurement the equilibration time has been several days and that is certainly sufficient for attainting steady state conditions.

The true average of the local mean age of air in the room may be estimated by averaging all measurement points (see Etheridge and Sandberg, 1996). These averages are shown in Figure 3 below. It seems that the first measurement set gives a higher estimate than the other three measurements, which may be a further indication that the waiting time before measurement might have been too short.

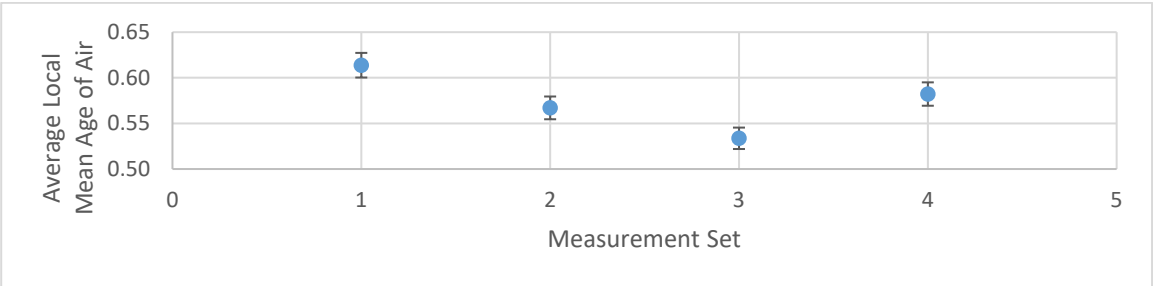

Figure 3. The measured local mean age of air for all measurements.

To estimate the transfer probabilities due to aerosol transport from the source of an infected occupant to the measuring positions, the relative apparent emission rates are shown in Figure 4. (Note that the datapoint numbers in Figures 4-7 correspond to the numbers given for sampler positions in Figure 1.) The relative standard error in the relative apparent emission rates is estimated to be 15 %. Note that this is the steady state transfer probability that is

established over a longer period. Also note that there is a diagonal symmetry, in relation to the exhaust, in the laboratory setup in Figure 1a. In mixing ventilation condition, the red and yellow manikins are expected to experience similar environments. The environments of the green and blue manikins should also be similar but may differ from those of the red and yellow manikins.

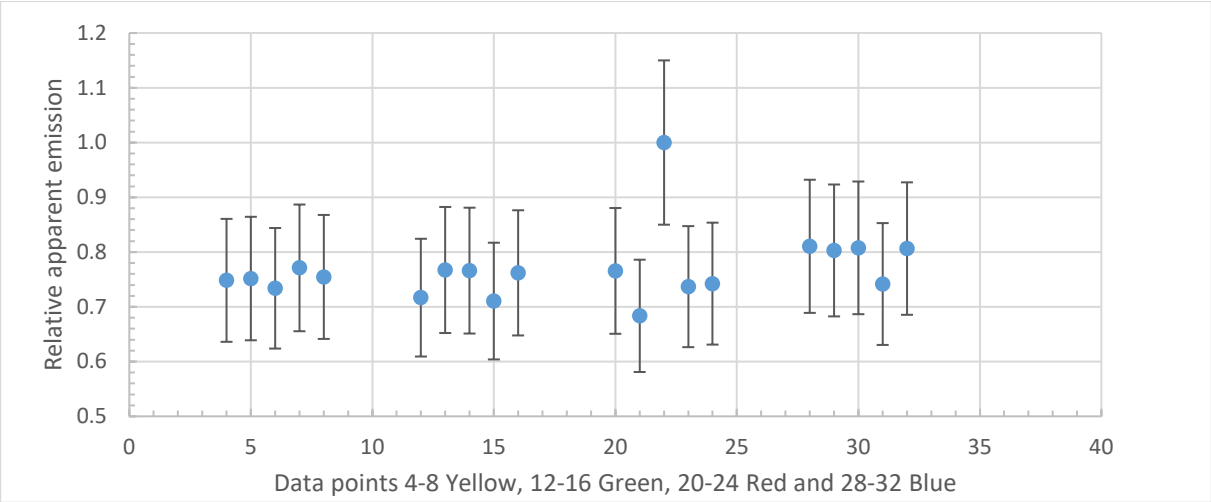

Figure 4. The relative apparent emission for the first measurement (B source in the Red breathing zone). Note that the data are presented according to height above the floor for each color: 0.5 m and 1.0 m (on the string behind the manikin), 1.1 m (in the breathing zone of the manikin), then 1.5 m and 2.0 m (on the string behind the manikin).

The transfer probability the red breathing zone (see Figure 1a) is fairly uniform as seen in Figure 4. The average transfer probability is 0.76 ± 0.03 (mean ± std). The two manikins closer to the exhaust (i.e. green and blue) are slightly boosted by the biased results for the local mean age of air that was noted in Figure 2.

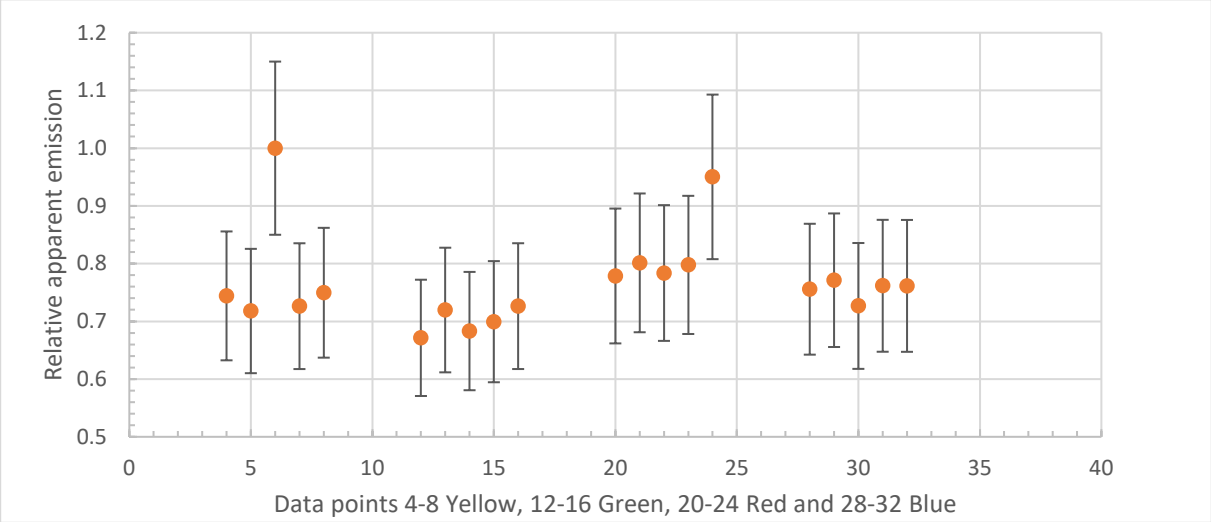

Figure 5. The relative apparent emission for the second measurement (B in Yellow). Note that the data are presented according to height above the floor for each color: 0.5 m and 1.0 m (on the string behind the manikin), 1.1 m (in the breathing zone of the manikin), then 1.5 m and 2.0 m (on the string behind the manikin).

Figure 5 shows the relative apparent emission rates for the case where the B source is placed in the yellow breathing zone (see Figure 1a). The values related to the red manikin show higher transfer probabilities. This effect might be real, but there is also a risk that carry-over effects are observed between the experiments since the B-tracer was placed by the red manikin in the experiment before. Carry-over effects may be due to possible adsorption in the manikin fabric or too short waiting time between the measurements. The transfer probabilities related to the blue manikin are slightly larger than those for the green manikin. The average transfer probability is 0.75 ± 0.06.

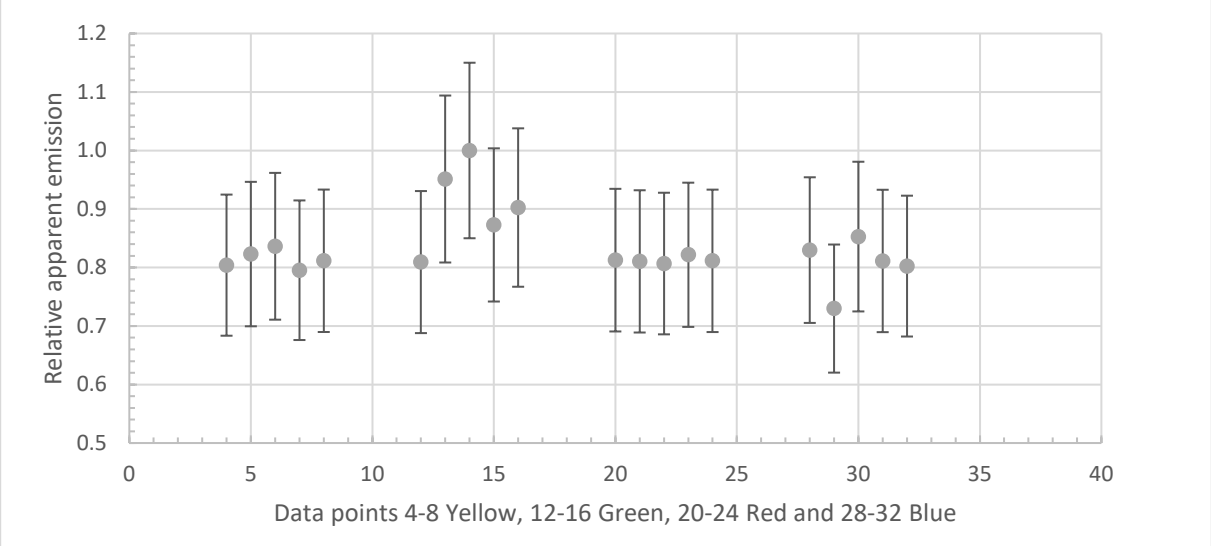

Figure 6. The relative apparent emission for the first measurement (B in Green). Note that the data are presented according to height above the floor for each color: 0.5 m and 1.0 m (on the string behind the manikin), 1.1 m (in the breathing zone of the manikin), then 1.5 m and 2.0 m (on the string behind the manikin).

The transfer probabilities when the B-tracer is placed in the green breathing zone are shown in Figure 6. There may be carry-over effects for the yellow manikin, but it is less clear since the results are similar för the red and blue manikin. The results are quite uniform and higher than the two previous cases. The average transfer probability is 0.83 ± 0.04.

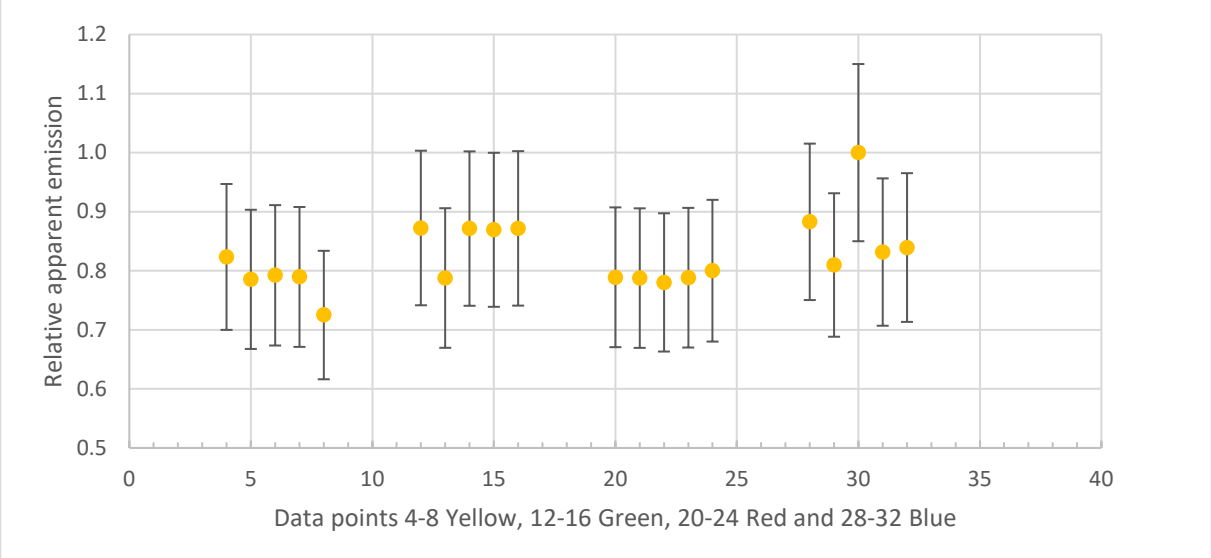

Figure 7. The relative apparent emission for the first measurement (B in Blue). Note that the data are presented according to height above the floor for each color: 0.5 m and 1.0 m (on the string behind the manikin), 1.1 m (in the breathing zone of the manikin), then 1.5 m and 2.0 m (on the string behind the manikin).

In Figure 7, the relative apparent emission for the case where the B-tracer is placed in the blue breathing zone. The transfer probabilities related to the green manikin are slightly higher than those of the red and yellow manikins. This observation may be due to real effects but may also be carry-over effects. The average transfer probability is 0.82 ± 0.04. It is higher than those observed for the red and yellow breathing zones and almost as high as for the blue breathing zone.

5 CONCLUSIONS

The methods used appear to provide consistent and plausible results for the present laboratory setup when the heat sources for the manikins are off. The relative apparent emission rates that are calculated from the measurements may in fact be measures of the steady state transfer probabilities of air packages containing infectious aerosols within the office space. The diagonal symmetry of the setup suggested that the local environment for the red and yellow manikin pair should be similar. The same could be said for the green and blue manikin pair. This indeed what is seen to a slight extent. The observed steady state transfer probabilities from the breathing zones of the green and blue manikin are 0.83 ± 0.04 and 0.82 ± 0.04, respectively. The corresponding results for the red and yellow breathing zones are 0.76 ± 0.03 and 0.75 ± 0.06. As expected, for mixing ventilation conditions, the steady state probabilities to most positions are similar. Nevertheless, the transfer probabilities from the breathing zones of the manikins closer to the exhaust cause slightly more spreading. This is somewhat counterintuitive and warrants further investigations.

6 ACKNOWLEDGEMENTS

I would like to thank Alan Kabanshi and his group for allowing me to perform the measurements in their laboratory setup. Elisabeth Linden is acknowledged for help with practical details.

7 REFERENCES

Björling M, Mattsson M.; Blomberg C, Stymne H. Ventilation Measurements Combined with Pollutant Concentration Measurements Discriminates Between High Emission Rates and Insufficient Ventilation. IAQVEC 2007 Indoor Air Quality Ventilation and Energy Conservation: Sustainable Buildings. P. 2, Sendai, Japan, 2007, 402-409

Etheridge DW, Sandberg M. Building ventilation: theory and measurement. Chichester: Wiley; 1996.

ISO-standard, ISO 16000-8, “Determination of local mean ages of air in buildings for characterizing ventilation conditions”, 2007-06-15.

Kabanshi A, Andersson H, Sundberg M, Senkic D, Sandberg M. Assessing airborne infection risk through a model of airflow evacuation and recirculation dynamics. RoomVent 2024: Healthy air together - when scientific and industrial advances meet the needs of society, April 22-25, Stockholm, Sweden. Conference Proceedings.

Kurnisky J, Kiil M, Mikola A, Vösa KV, Aganovic A, Schild P, Seppänen O. Post-COVID ventilation design: Infection risk-based target ventilation rates and point source ventilation effectiveness. Energy & Buildings 296 (2023) 113386.

Sandberg M. Ventilation effectiveness and purging flow – a review. International Symposium on Room Air Convection and Ventilation Effectiveness, Tokyo, Japan, 1992.

Wagner J, Sparks TL, Miller S, Chen W, Macher JM, Waldman JM. Modeling the impacts of physical distancing and other exposure determinants on aerosol transmission, J. Occup. Environ. Hyg. 18 (2021) 495–509.
Zhang, S., Lin, Z., 2021. Dilution-based evaluation of airborne infection risk-Thorough expansion of Wells-Riley model. Building and Environment 194, 107674.